JOURNAL OF MATERIALS SCIENCE **34** (1999) 195–208

Microstructural characterization of grain-oriented glass-ceramics in the system $Ba_2TiSi_2O_8$ - SiO_2

T. HÖCHE, R. KEDING, C. RÜSSEL
Otto-Schott-Institut für Glaschemie, Friedrich-Schiller-Universität Jena, Fraunhoferstrasse 6, D-07743 Jena, Germany
E-mail: hoeche@glas.chemie.uni-jena.de

R. HERGT
Institut für Physikalische Hochtechnologie e.V., Helmholtzweg 4, D-07743 Jena, Germany

In polycrystalline fresnoite, advantage of the piezo- and pyroelectric properties can be taken only if texturing along its polar [0 0 1]-axis can be achieved. We report on a novel technique to prepare grain-oriented glass-ceramics in the system fresnoite-SiO_2 by electrochemically induced nucleation. Optimum conditions for grain orientation were determined by characterizing the microstructure of glass-ceramics prepared at 1150, 1200 and 1350 °C using electron microscopy and X-ray texture goniometry. At 1150 °C—due to the smallest crystal growth rate and highest nucleation rate—the most distinct orientation is obtained. The solidification of the glass-ceramic consist of three subsequent steps. First, dendritic fresnoite crystallizes most rapidly along its [0 0 1]-axis with {1 1 0} facet planes. Due to growth selection, the polar *c*-axes become oriented. Secondly, within the interdendritic areas, the pseudo-binary eutectic fresnoite-silica solidifies lamellarly. Finally, in the middle of the interspaces, a crystalline barium silicate coexisting with glassy silica is formed at 1200 °C and 1350 °C. At 1150 °C, however, a glass with the composition of the melt solidifies.

1. Introduction

In 1965, during geologic studies of sanbornit deposits in eastern Fresno County, CA, a new barium silicate mineral was found and named fresnoite, $Ba_2TiSi_2O_8$ [1]. Subsequently, the space group of fresnoite was determined to be P4bm [2, 3]; lattice parameters of $a = 0.8529$ nm and $c = 0.5211$ nm and a density of $\varrho = 4.43$ g cm^{-3} were found [4, 5]. The co-ordination of titanium in the fresnoite structure is remarkable, since it is located inside square pyramids, i.e. the co-ordination is five-fold. These TiO_5 groups are edge-linked with pyrosilicate groups resulting in sheets perpendicular to the [0 0 1]-direction. Ten-fold oxygen co-ordinated barium ions are located between these sheets in the center of slightly distorted pentagonal antiprisms. The peculiar titanium co-ordination results in permanent electrical dipoles along the [0 0 1]-axis.

Due to its acentric structure, fresnoite possesses polar properties: $Ba_2TiSi_2O_8$ is piezoelectric [6] as well as pyroelectric [7, 8] and shows non-linear optical effects [9]. Although fresnoite contains permanent electric dipoles, it is not ferroelectric since the dipoles are not switchable. All elastic constants, their temperature coefficients, the thermal-expansion coefficients and also the piezoelectric constants of grown single-crystals were determined [10, 11]. Due to high values of the hydrostatic piezoelectric coefficient and the hydrostatic voltage coefficient, as well as a rather low dielectric constant, fresnoite turned out to be a promising candidate for hydrophon and other piezoelectric applications [12–14].

Since its permanent dipoles cannot be reoriented by applying high electric field strengths, fresnoite is of little use as a polycrystalline ceramic unless polar axes are oriented. It is therefore necessary to develop technologies for orienting the polar axes during crystallization. In the literature, until now, three ways to crystallize oriented $Ba_2TiSi_2O_8$ glass-ceramics are reported. The first method applies a steep temperature gradient of approximately 100 K mm^{-1} which results in the growth of needle-like crystals of [0 0 1] orientation along the direction of the gradient [15]. The second alternative consists of a superficial ultrasonic treatment of glassy fresnoite with an aqueous suspension of fresnoite crystallites prior to a subsequent heat treatment (highly *c*-axis oriented films of about 50 μm thickness were obtained) [16]. Last, but not least, films of oriented fresnoite were grown on silicon substrates utilizing radio-frequency sputtering. A film thickness of up to 2.8 μm was achieved at substrate temperatures of 845 °C [17].

In this paper, we report on an alternative means to achieve grain orientation. As already reported briefly [18], oriented growth can be initiated by the flow of an electric current through the supercooled melt. In this study, we characterize the microstructure of the resulting highly grain-oriented fresnoite glass-ceramic.

Two imaging techniques with spatial resolutions covering several orders of magnitude (scanning electron microscopy, SEM, and transmission electron microscopy, TEM) were used to obtain a detailed insight into the microstructure. The composition of the phases observed was analyzed using energy dispersive X-ray analysis (EDX) in the transmission electron microscope. Moreover, the application of X-ray texture goniometry allows for a generalization of the results obtained by imaging techniques.

On the basis of the observed microstructure, nucleation and growth mechanisms as well as possible improvements of the microstructure are discussed.

2. Experimental

2.1. Specimen preparation

Using $BaCO_3$ (Merck), TiO_2 (rutile, Merck, optipur) and SiO_2 (quartz), a melt of the composition $Ba_2TiSi_2O_8 \cdot 0.75\ SiO_2$ was prepared in an inductively heated furnace. The platinum crucible (250 ml) was heated to 1550 °C and the melt was homogenized by stirring for two hours and subsequent soaking for another two hours.

For electrochemically induced crystallization, the crucible was connected to the positive pole of an electrical current supply (anode), whereas a platinum cylinder or wire contacted to the negative pole of the current supply was introduced into the melt in the middle of the crucible (cathode). The melt was carefully supercooled by several hundred Kelvin. After adjusting to a temperature of either 1150 °C, 1200 °C or 1350 °C, at an initial voltage of about 1.2 V, a current of 50 mA was allowed to pass through the supercooled melt for a few minutes (the current–voltage characteristics are discussed elsewhere [19]). Immediately upon applying the electrical current, crystallization of the melt could be observed starting from the cathode.

Due to a temperature gradient parallel to the cathode axis, crystallization tends to start form the surface of the melt. As approved by inserting a thermocouple, superficial parts of the melt—being in contact with the surroundings—are approximately 50 K colder than inner parts, whereas temperature differences between the center and the periphery of the melt are negligible. The temperature distribution is much more homogeneous if the crucible is covered with an alumina plate.

After about ten minutes (the higher the temperature, the faster the growth velocity), the melt was completely crystallized. In practice, the already crystallized part of the melt was retracted from the remaining liquid just before the solidification front reached the crucible walls. Subsequently, the solidified glass-ceramic was rapidly transferred into a furnace for a very slow and definite cooling to room temperature.

Specimens were embedded in an epoxy resin (Araldite CY 212, Agar Scientific) to improve mechanical stability for further processing. Slices perpendicular to the cathode axis were cut using a diamond saw; faces were ground and polished to optical quality.

TEM samples were prepared by subsequent plane-parallel grinding and polishing to about 100 μm thickness, cutting of 3 mm disks using an ultrasonic disk cutter, one-sided dimpling to a residual thickness of about 20 μm and finally ion beam etching at 2.0 to 2.5 kV acceleration voltage and beam currents (Ar^+) of about 0.8 mA. Such fairly low values of both acceleration voltage and beam current together with the low

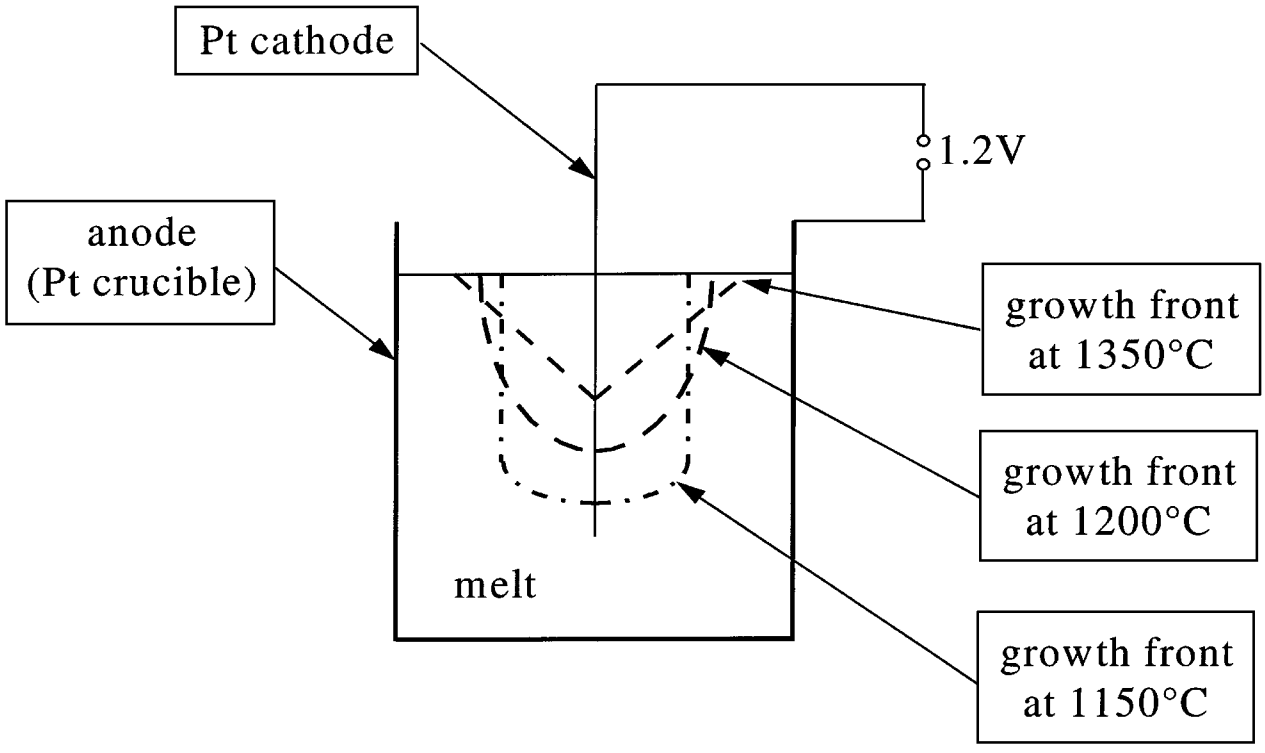

Figure 1 Schematic drawing of the growth bodies formed at crystallization temperatures of 1150, 1200 and 1350 °C together with the experimental set-up.

incidence angle of 6° were applied to avoid preparation artefacts. To protect both TEM foils and SEM samples from static charging under the electron beam, a thin layer of amorphous carbon was deposited on them.

2.2. Methods of characterization

For X-ray texture goniometry an Xpert X-ray diffractometer (Philips) was used. Scanning electron microscopy was performed in a Zeiss DSM 940A. For TEM, a Hitachi H-8100 II electron microscope operated at 200 kV acceleration voltage (point-to-point resolution 0.23 nm) was used. Spectra for microprobe X-ray analyses were acquired using a Link Isis (Oxford Instruments) X-ray spectrometer with an ultra-thin window fitted to the H-8100 II.

3. Results

Three samples—corresponding to three different temperatures of crystallization: 1150 °C, 1200 °C as well as 1350 °C—were characterized. As depicted in Fig. 1, the shape of the growth front depends on the temperature of crystallization. In the sample prepared at the highest temperature (1350 °C), the growth front resembles a low cone, whereas in the sample crystallized at 1150 °C the shape is almost cylindrical but slightly tapered to a point at the lower tip. The correlation of the growth habits with the microstructure and the microstructure itself will be examined in the following.

3.1. Sample crystallized at 1150 °C

Fig. 2, a micrograph taken in the SEM, gives an insight into the microstructure of the fresnoite glass-ceramic.

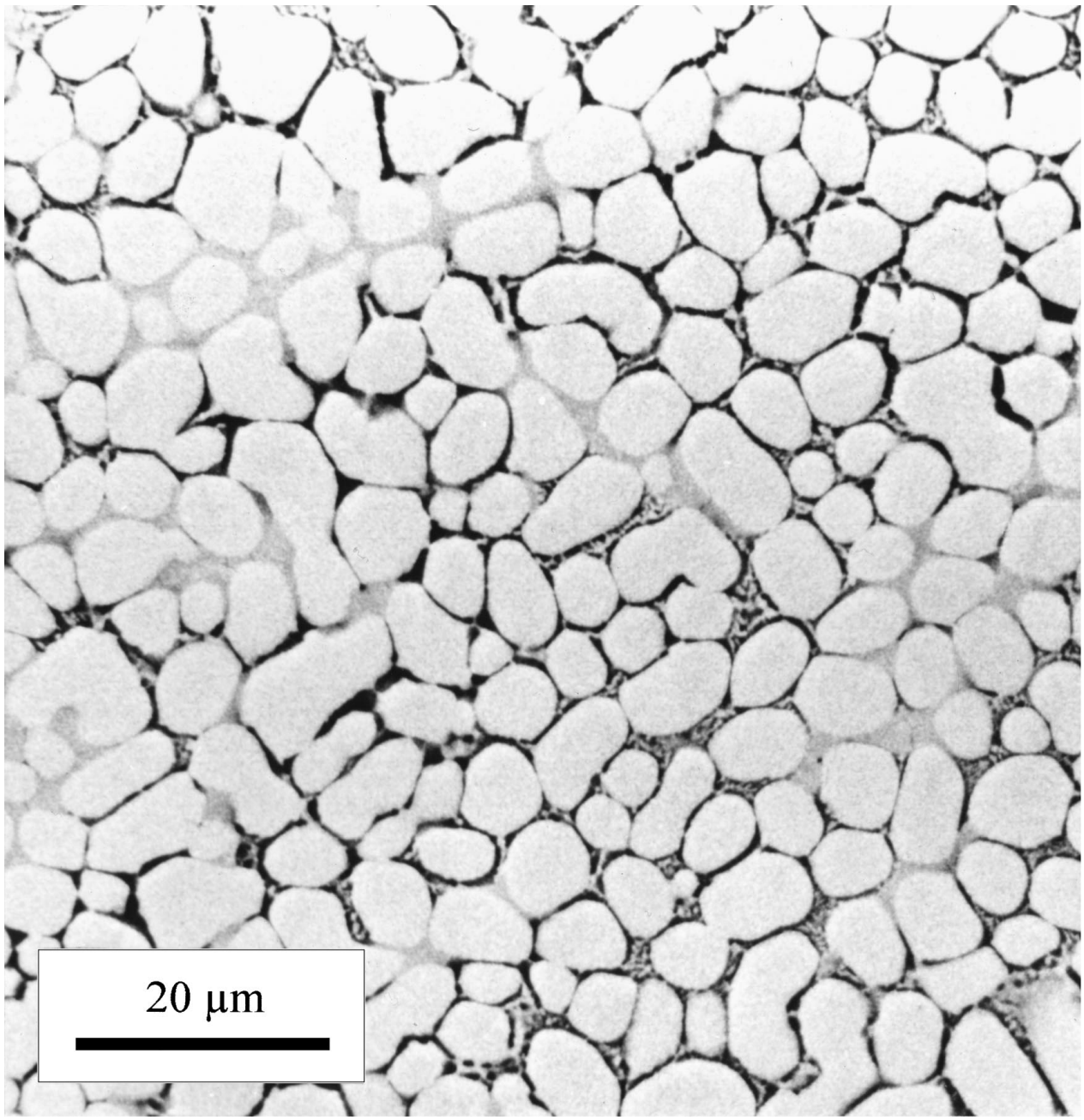

Figure 2 SEM overview (back-scattered electrons) showing the microstructure in the sample solidified at 1150 °C. Branches of dendritic fresnoite appear light grey and glassy silica black. The branch diameters have a narrow size distribution with an average of about 10 μm.

The specimen was cut perpendicular to the cathode axis in the upper part of the sample (cf. Fig. 1). As shown by electron diffraction in the TEM, the [0 1 0]-axis of the bright grains (dendritic fresnoite) is within some degrees perpendicular to the plane of the paper. All grains of dendritic fresnoite are interconnected in the direction of projection and therefore possess a common orientation. In the upper left part of Fig. 2, as a result of the excitation depth in SEM (a few micrometers), bridging of grains that are in fact dendrite branches is indicated (interspaces appear light grey rather then black). Branches have diameters between two and some ten micrometers.

The TEM micrograph in Fig. 3 reveals that the interspaces between the branches of dendritic fresnoite consist of indicated lamellae with distances of about 1 μm. As shown by EDX spectroscopy, layers of glassy silicon oxide and fresnoite alternate. In the middle of such interspaces, a third remainder phase can be found (marked QM in Fig. 3). Due to the small excitation volume, the identification of this phase should be possible in the TEM. Unfortunately, in analyzing EDX spectra, the distinction between barium and titanium is difficult—particularly for small concentrations of only one of the elements—due to peak overlap (the energy difference between $E(\mathrm{TiK}_{\alpha 1}) = 4.510$ keV and $E(\mathrm{BaL}_{\alpha 1}) = 4.467$ keV amounts $\Delta E = 43$ eV; this is much smaller then the energy resolution of 142 eV (defined at the energy of the MnK_{α} line, $E = 5.898$ keV) of the spectrometer used). Therefore, electron energy loss spectroscopy (EELS) (which is able to undoubtedly differentiate between barium and titanium) was used to determine the composition of this phase. EELS data confirmed that this phase does contain barium, titanium, silicon as well as oxygen (a detailed analysis of the EEL spectra will be given elsewhere [20]). By electron micro-diffraction, this remainder phase was proved to be glassy. Using Kikuchi patterns, the relative orientation of the fresnoite grains along the hole in the TEM samples was analyzed (in contrast to diffraction patterns

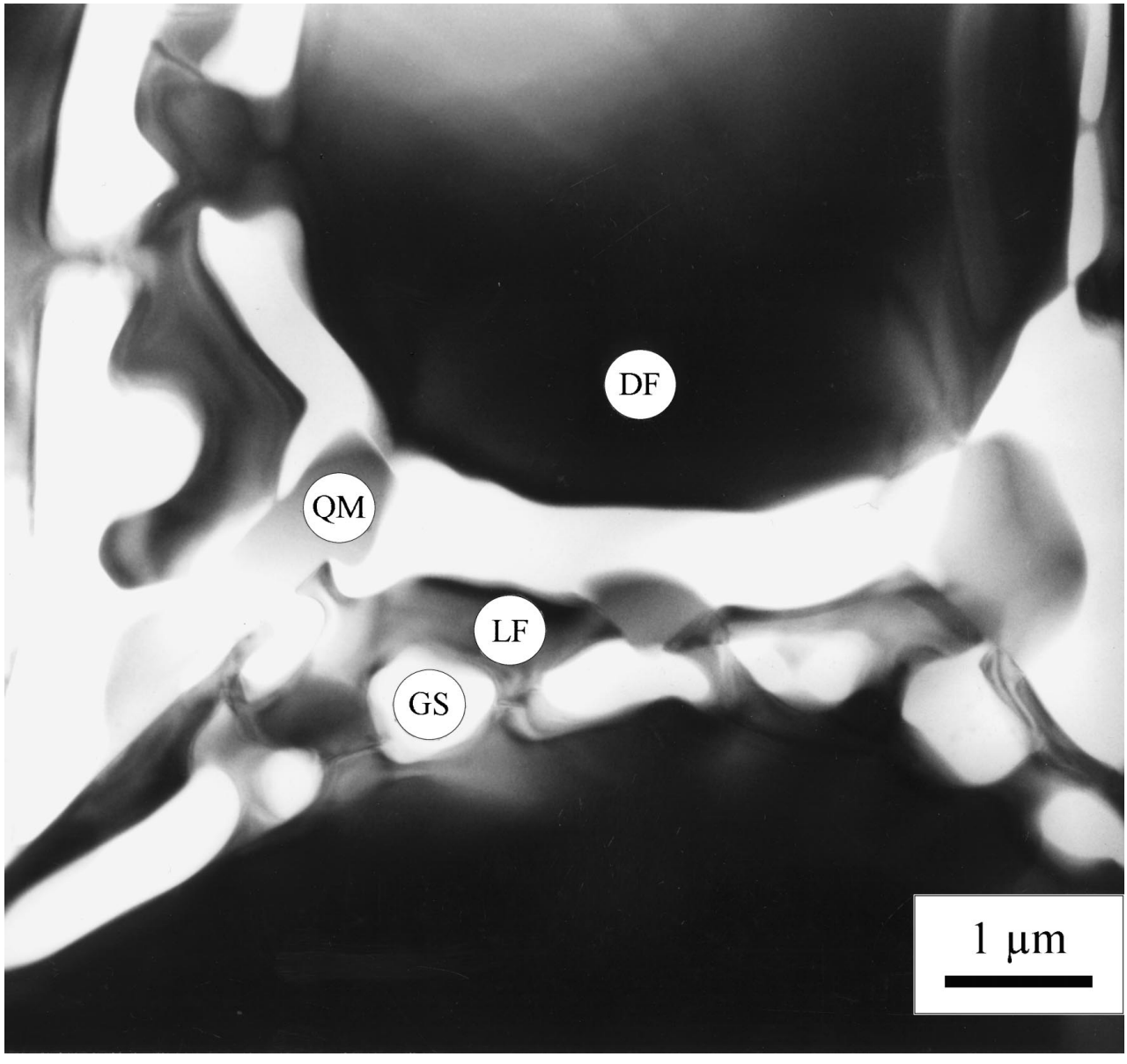

Figure 3 TEM micrograph showing branches of dendritic fresnoite (DF), initial states of alternating layers of crystalline lamellar fresnoite (LF) and glassy silica (GS) as well as a quenched melt (QM). Bending contours inside the lamellar fresnoite indicate epitaxial intergrowth of dendritic and lamellar fresnoite.

which are influenced by excitation errors and therefore the shape of the specimen, Kikuchi patterns are firmly fixed on the crystal lattice). At typical hole diameters of a few tenths of a millimeter (e.g. in most cases only one orientation domain is in the field of view) along the electron-transparent part of the specimen orientation, deviations up to about 8° are to be observed (this value might be influenced by local bending of the TEM foil arising from the preparation). Changes in orientation are small and continuous inside dendritic domains but abrupt between neighboring domains.

Furthermore, specimens cut at different heights of the sample (cf. Fig. 1) were investigated. The first of these TEM foils was prepared from the upper part of the sample (near the surface of the melt) 5 mm apart from the cathode. Electron diffraction revealed the [0 1 0]-axis of fresnoite dendrites to be parallel to the cathode. The *c*-axis is pointing outwards in the radial direction. The second of these TEM foils originated from the lower end of the cathode. The hole in the TEM specimen had a radial distance from the cathode of about 1 mm. Here, the [0 0 1]-axis of fresnoite was approximately perpendicular to the cathode axis. The third specimen was taken from the same cut perpendicular to the cathode axis, but at a radial distance of about 6 mm. Surprisingly, within the experimental uncertainty of some degrees, the [0 1 1]-axis rather then the [0 0 1]-axis of the dendritic fresnoite was parallel to the cathode wire. Since the angle between [0 0 1] and [0 1 1] is 31.42°, it can be concluded that the orientation of the *c*-axis with respect to the cathode axis is changing with depth as well as with distance from the cathode. The *c*-axis is running in the radial direction in the upper part of the sample and becomes subsequently parallel to the cathode axis at and below the lower end of the cathode wire.

3.2. Sample crystallized at 1200 °C

Fig. 4 depicts the microstructure of the sample crystallized at 1200 °C consisting of main branches (that are cut approximately parallel to the [0 0 1]-axis and run in the vertical direction) and smaller twigs that branch off laterally. In comparison to the sample prepared at 1150 °C, dendritic branches are similarly sized. Fresnoite dendrites no longer possess circular, elliptical or horseshoe-shaped cross-sections (viewed along the *c*-axis) without any sharp edges as observed in samples crystallized at 1150 °C, but show much better developed edges and indications of initial states of the formation of patterns that resemble angular spirals in the sample grown at 1350 °C. As proved by electron diffraction, the major faceting plane is of the {1 1 0}-type.

In Fig. 5, showing the platinum cathode (in the lower right corner) and its vicinity, the *c*-axes run in a remarkable manner. They do not follow the electrical field

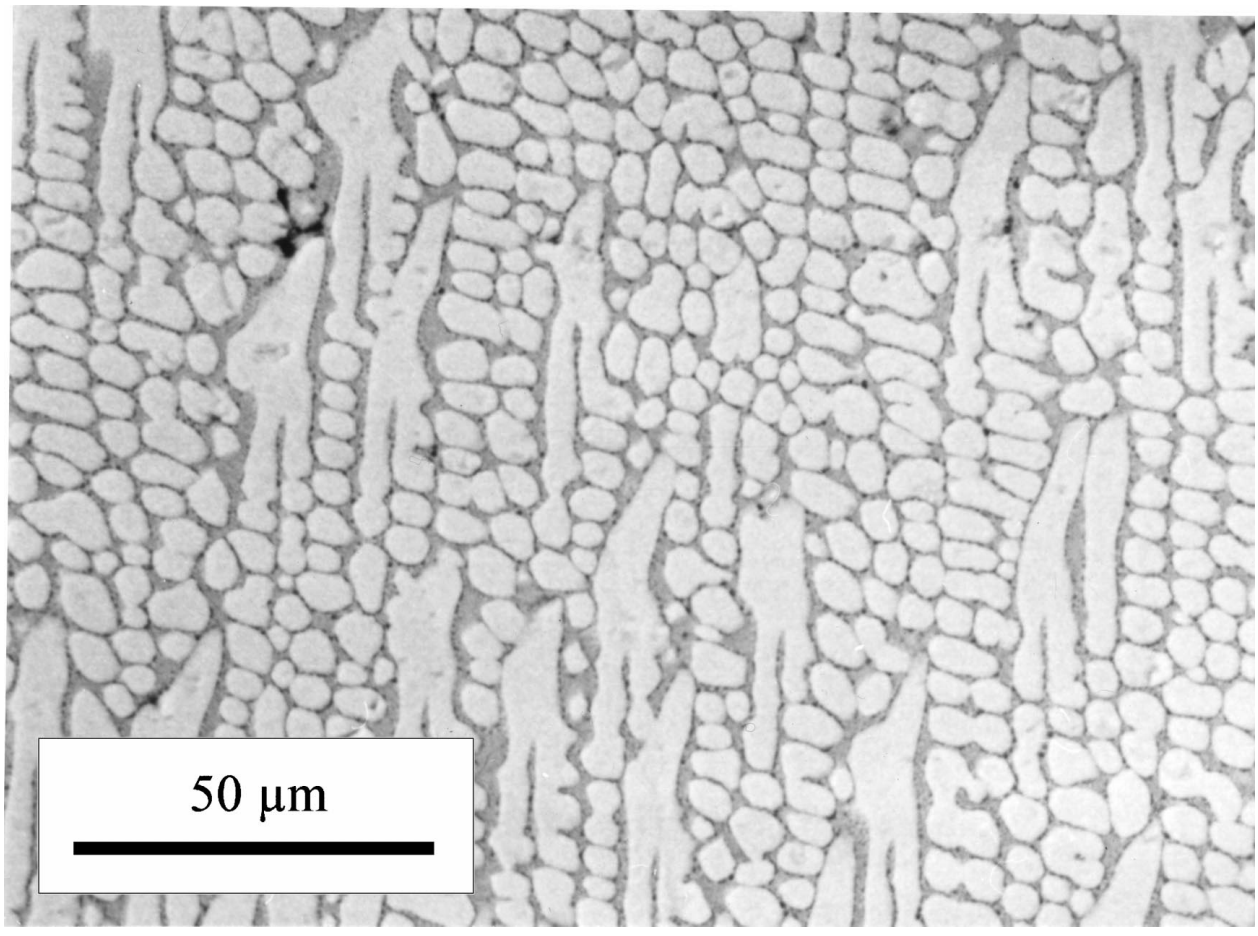

Figure 4 SEM overview (back-scattered electrons) showing the microstructure in the sample solidified at 1200 °C. The major growth direction [0 0 1] is running approximately vertically. Branches of dendritic fresnoite (which are cut almost parallel to their axes) appear light grey and glassy silica is black. The branch diameters have a narrow size distribution with an average of about 8 μm.

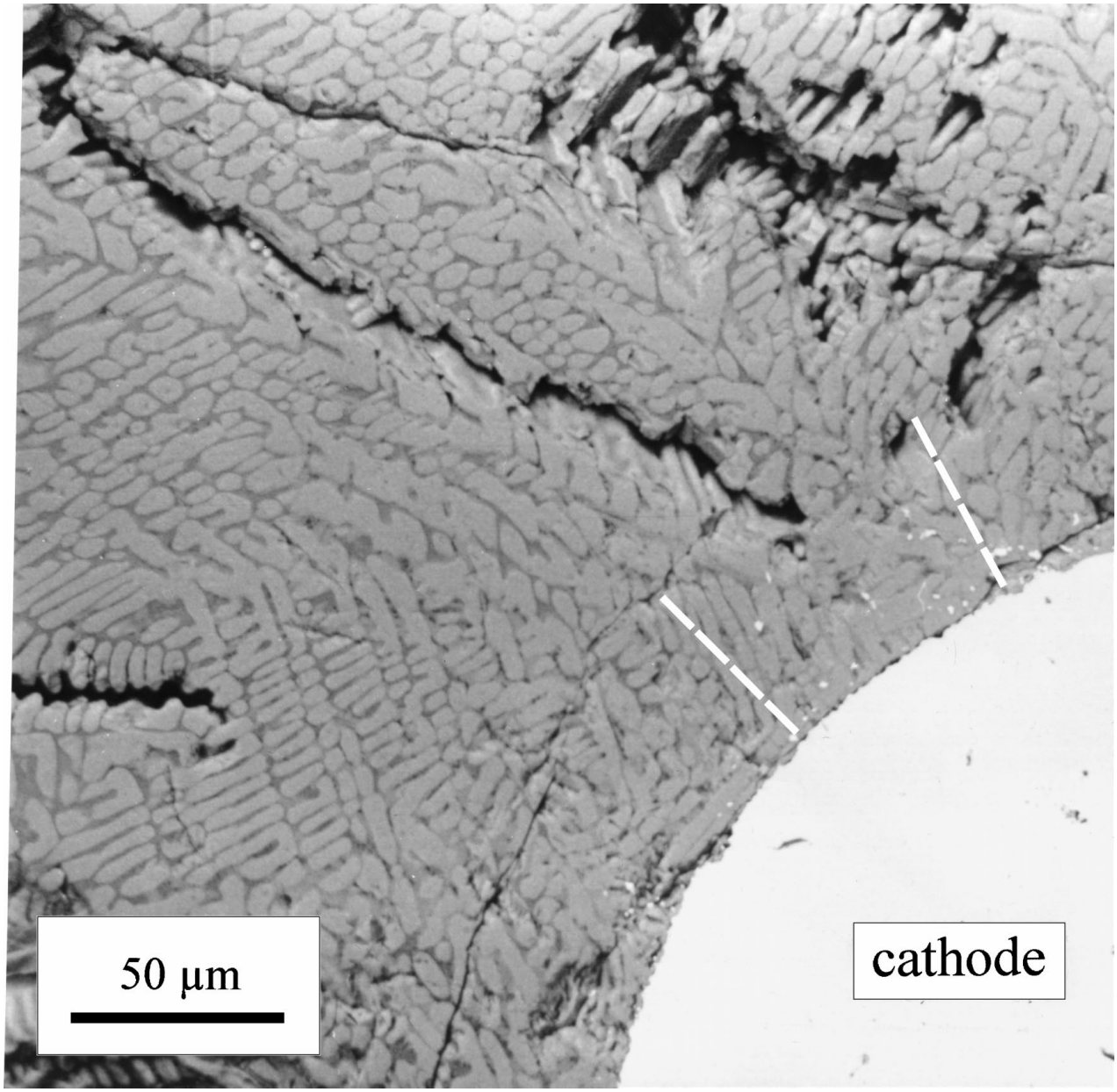

Figure 5 SEM micrograph depicting the immediate vicinity of the cathode (white circular sector in the lower right corner). The normal of the wire that corresponds to the electrical field lines is indicated by two dashed guide lines. The dendritic domains become more ordered with increasing distance from the cathode. Together with the fact that the growth direction deviates considerably from the direction of the electrical field this is interpreted in terms of growth selection taking place near the cathode.

which runs in the radial direction but seem to follow a tangency on the surface of the wire.

The interspaces between dendritic branches are filled with a eutectic that is lamellarly solidified with an average spacing of 0.35 μm (Fig. 6). Also in this sample, some residual phase is left in the middle of the interspaces between the dendrites. However, in contrast to the sample solidified at 1150 °C, this remainder is not glassy and, as proved by electron energy loss spectroscopy, it does not contain any titanium. A closer look at the microstructure (cf. Fig. 7) reveals that those parts of the sample consist of three different compounds: some fresnoite crystals growing epitaxially from the fresnoite lamellae, glassy SiO_2 and crystalline $Ba_5Si_8O_{21}$. The monoclinic inosilicate $Ba_5Si_8O_{21}$ (space group C2/c, $a = 3.270$ nm, $b = 0.470$ nm, $c = 1.390$ nm, $\beta = 98.144°$) was identified from its diffraction patterns as well as from HRTEM images that frequently show (0 1 0) and (1 0 0) fringes. Within the experimental errors, the composition of $Ba_5Si_8O_{21}$ agrees well with EDX analyses.

Analyses of Kikuchi patterns gave results comparable to those of the samples crystallized at 1150 °C.

3.3. Sample crystallized at 1350 °C

Visual inspection of the samples prepared at 1350 °C (cut perpendicular to the axis of the cathode) in the optical microscope revealed much larger dimensions of the domains in comparison to the samples discussed previously.

In Fig. 8a, the {0 0 2} Wulff plot of X-ray texture goniometry data obtained from a cut perpendicular to the Pt wire is depicted. Besides noting that the relative

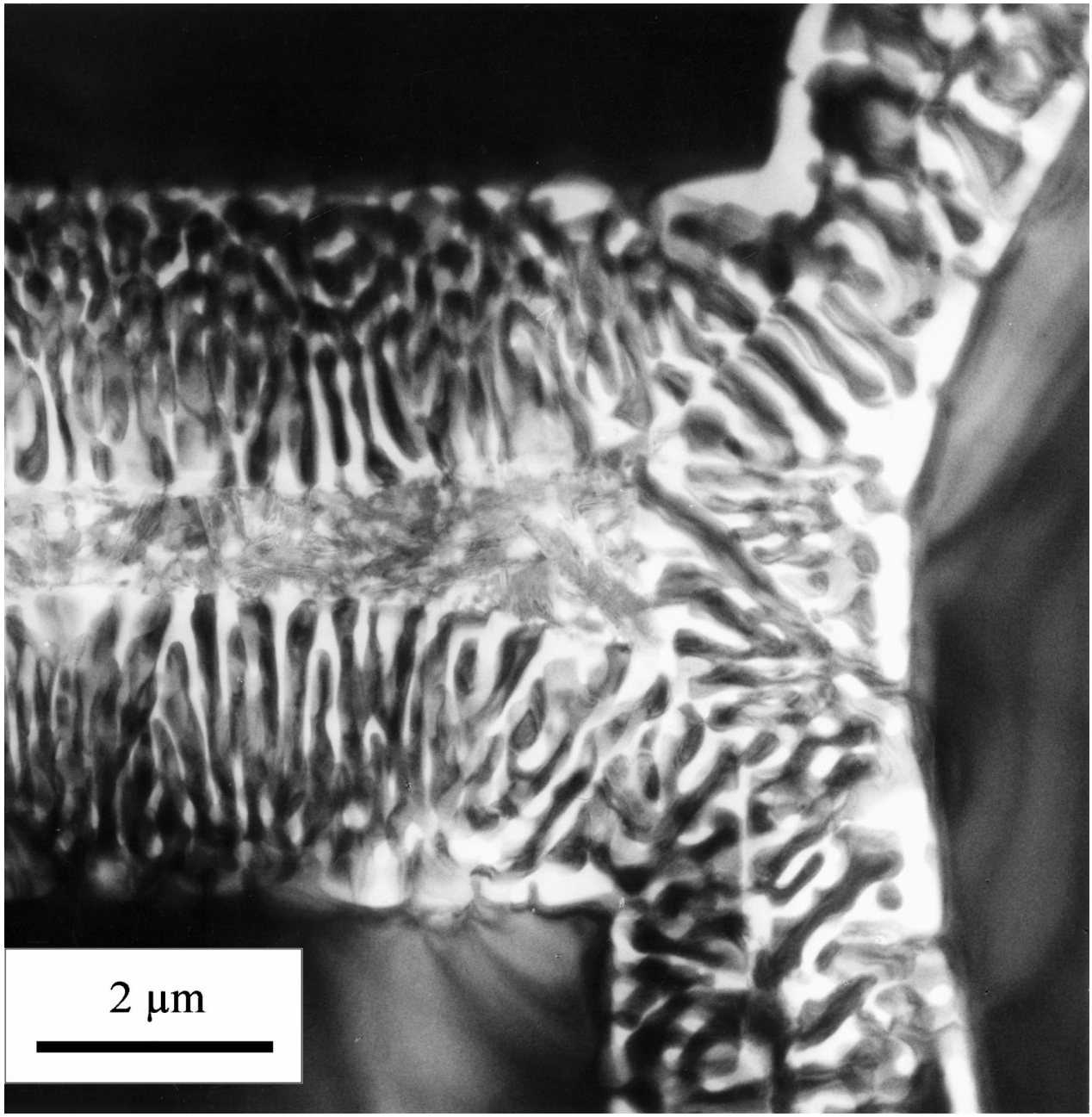

Figure 6 Sample prepared at 1200 °C: TEM insight into the interdendritic area consisting of the lamellarly solidified eutectic fresnoite-silica and a mixture of the crystalline barium silicate $Ba_2Si_8O_{21}$ and glassy silica in the middle. The fresnoite lamellae always grow perpendicular to the facet planes of dendritic fresnoite at an equilibrium spacing of about 0.35 μm.

orientation of the four included domains from the lower part of the specimen deviates only within 10° from the Pt wire axis, it is interesting to note that their respective *c*-axes span an azimuth range of about 45° with a constant relative departure of about 15°. All peaks have remarkably small half widths of a few degrees. But not only the *c*-axes are highly oriented. Fig. 8b comprises a {2 1 2} Wulff plot of the same area. Due to space group symmetry, eight equivalent peaks would be expected for a single crystal and, in fact, all of them are found and the strongest peaks have half widths of about 5°. Although near some of the peaks satellite peaks are starting to form, the orientation in this crystallographic direction perpendicular to the *c*-axis is impressive.

As depicted in Fig. 9, the shape of fresnoite dendrites shows a much stronger tendency to form squared spirals. It is also remarkable that the platinum wire (bright circular spot in the middle) is entirely embedded in fresnoite dendrites belonging to the same orientation domain. Obviously, nucleation at lower parts of the cathode is not effective at all, so that a growth front approaching from the top just enclosed the wire with solidified fresnoite glass-ceramics.

Also in this sample (cf. Fig. 10), some partly crystalline remainder solidifies in the middle of the 0.20 to 0.25 μm spaced lamellae consisting of crystalline fresnoite and glassy silica (Fig. 11). The amount of the remainder—containing only phases already found in the sample fabricated at 1200 °C—appear to be slightly increased in comparison with the 1200 °C sample.

High-resolution TEM was applied to illustrate something typical for all samples investigated in this study.

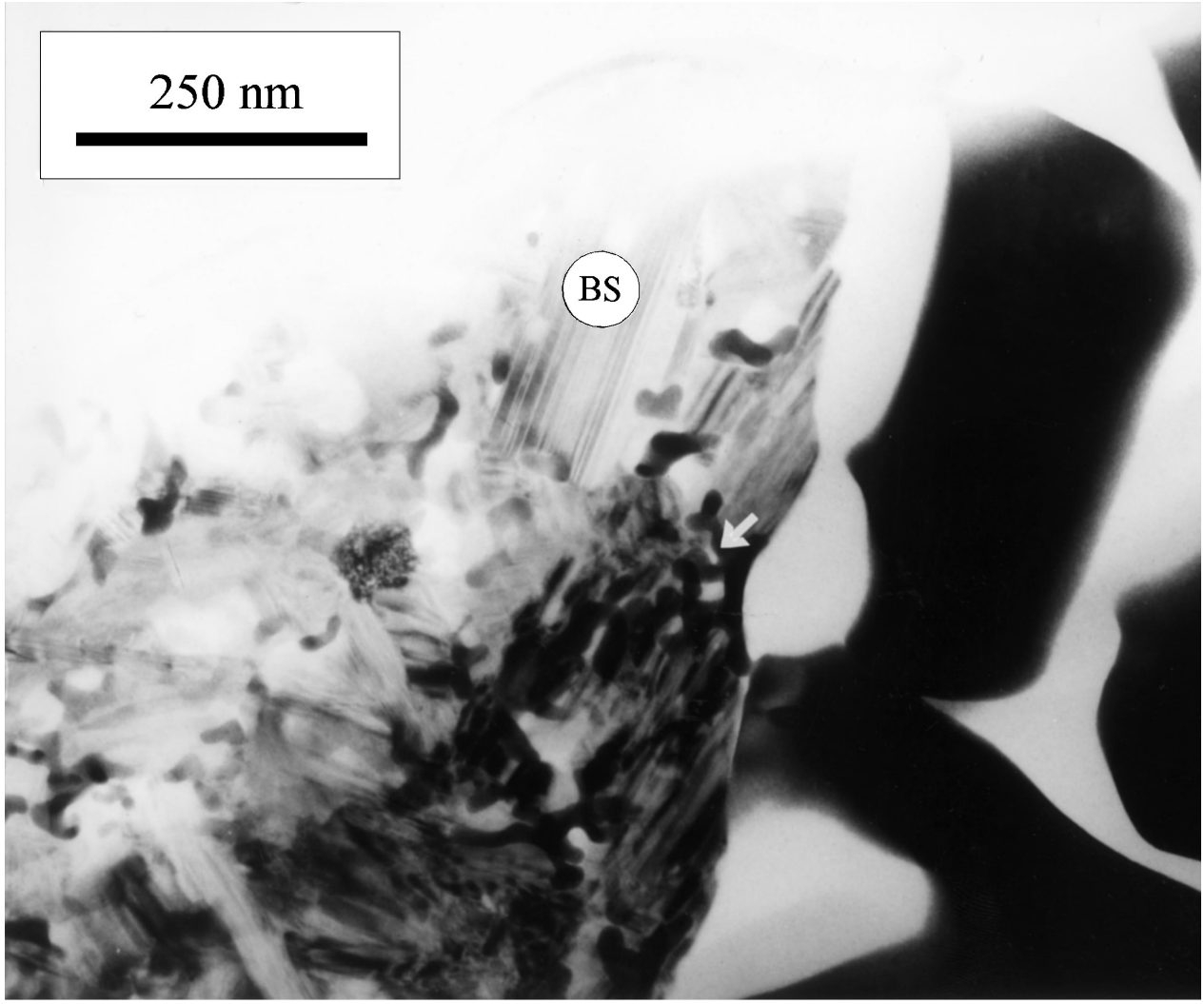

Figure 7 TEM micrograph showing the boundary between lamellar eutectic (right-hand side) and the remainder phase (left) in the middle of the interdendritic area. The transition is generally abrupt but occasionally some finely branching fresnoite can be observed (marked by an arrow). The sheet-like appearance of $Ba_5Si_8O_{21}$ (BS) is also to be seen clearly.

In Fig. 12, the necked region between a large fresnoite dendrite (right) and one of the fresnoite lamellae (left) attached to it is depicted. As proved by the undisturbed continuation of {1 0 0} and {1 1 0} lattice planes, both dendritic and lamellar fresnoite comprise a single crystal.

4. Discussion

The crystallization of fresnoite glass-ceramics under the influence of an electric current flowing through the supercooled melt is initiated by electrons transferred from the cathode into the melt. It is most likely that the reduction of Ti^{4+} to Ti^{3+} following the chemical equation: $Ti^{4+} + e^- \rightarrow Ti^{3+}$ is involved, although the detailed mechanism is still questionable.

During theoretical studies, it was concluded that the reduction may result in three effects, all suitable to increase the nucleation rate and to decrease the non-steady state time lag. First, the viscosity is decreased due to the occurrence of Ti^{3+} because it possesses more network forming properties than Ti^{4+}. The second effect is a change in the surface energy of the nuclei in contact with the melt, also caused by the incorporation of Ti^{3+} instead of Ti^{4+}. The extent of this effect can hardly be estimated, however, relatively small changes in the surface energy lead to drastic changes of nucleation rates. The third effect is an increase of the jump frequency of titanium due to the higher mobility of Ti^{3+}. At the moment, it is not possible to decide which effect is predominant, but all three may contribute to the increase in nucleation rate and decrease in non-steady state time lag. Finally, resolving the mechanism requires additional experiments and is the subject of continued investigations.

Seeds formed at the cathode grow most rapidly along the fresnoite *c*-axis. This is most obvious in the sample solidified at 1350 °C. Its upper part shows a radial orientation of the *c*-axes and in the lower part the crystallographic [0 0 1]-direction points parallel to the cathode wire. Being parallel to the surface in the uppermost part of the melt, [0 0 1]-axes are subsequently tilted towards the wire.

The outstanding degree of orientation is the result of crystal growth selection rather than growth following the direction of current flow. As depicted in Fig. 5,

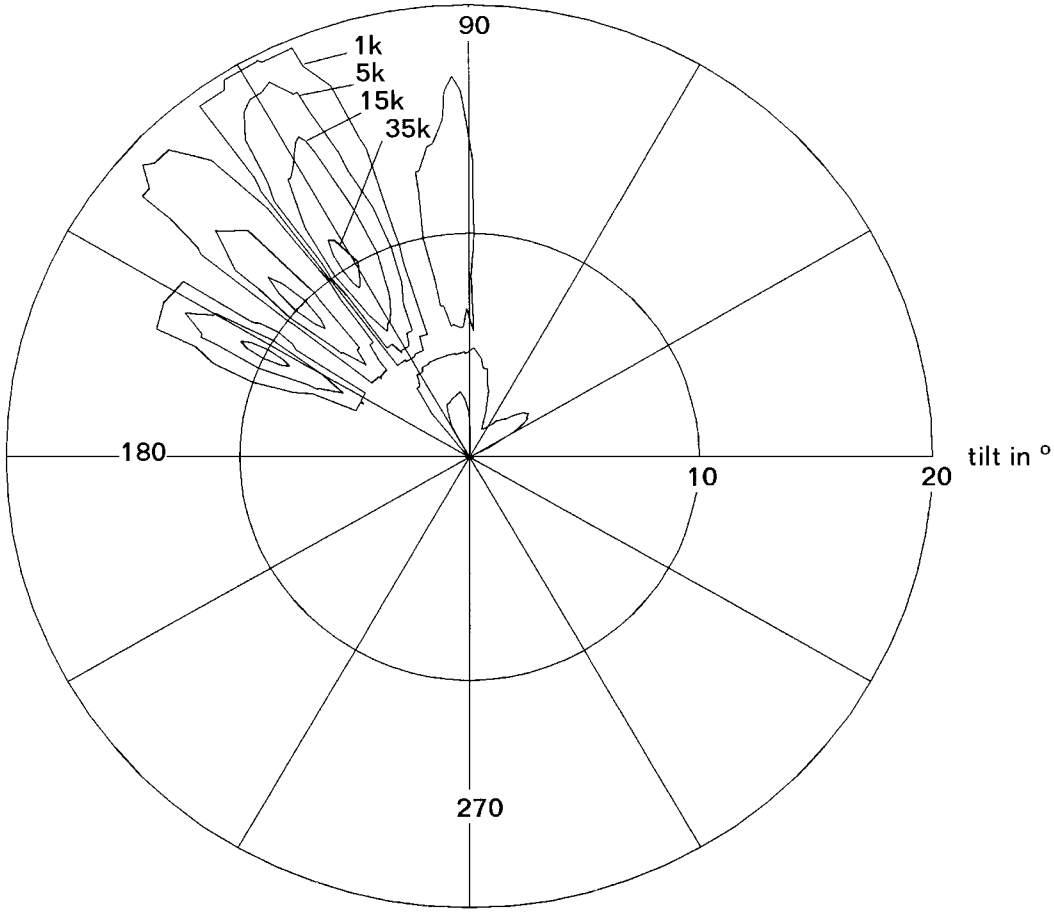

(a)

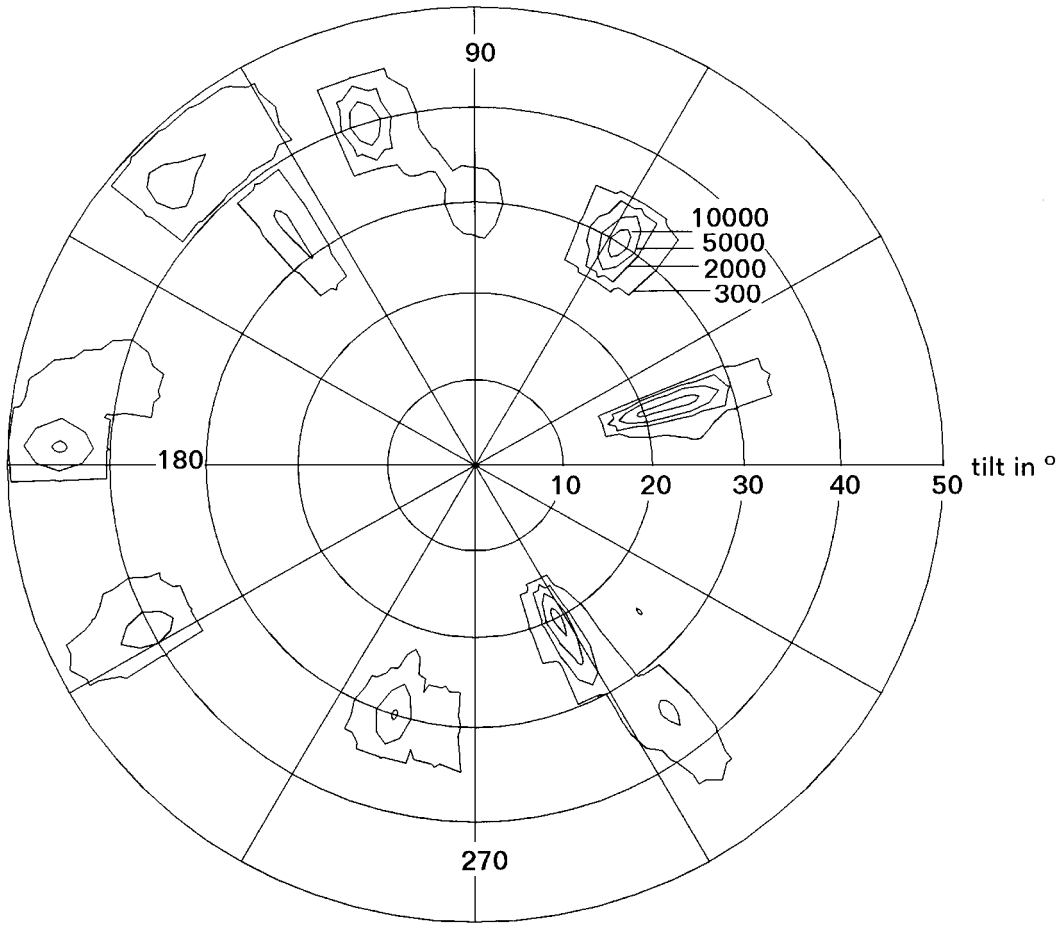

(b)

Figure 8 Wulff plots of X-ray texture goniometry data using: (a) (0 0 2) reflections and (b) (2 1 2) reflections. Note that the inner parts of the Wulff plots are depicted only because outer regions do not contain any peaks.

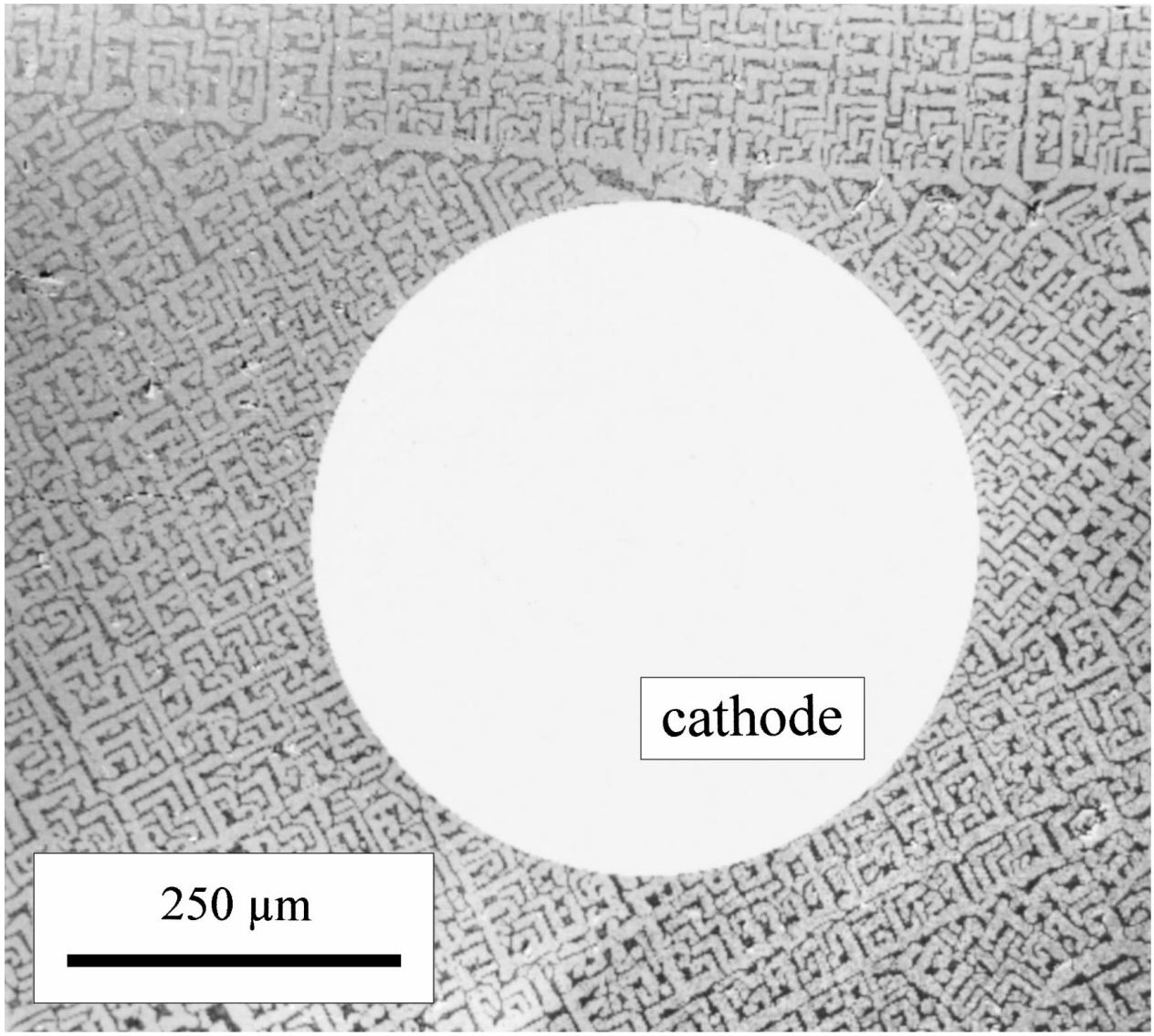

Figure 9 SEM overview (back-scattered electrons) showing a dendritic domain entirely embedding the cathode wire (white circle in the middle of the image) in the lower part of the sample crystallized 1350 °C. Fresnoite branches projected along [0 0 1] have a strong tendency to faceting along {1 1 0} planes and forms patterns resembling squared spirals. In this micrograph no indication of seed formation can be found.

the normal of the growth front is not correlated with the electrical field lines but differs considerably. Therefore, the highest degree of orientation could be obtained using a cathode wire instead of a cylinder of about 5 mm diameter (here, radial selection starts at larger radii).

As proved by X-ray texture goniometry, grain orientation is not only found in the direction of growth. A common orientation is observed also perpendicular to the *c*-axis. This can be explained in the framework of growth selection. Fresnoite dendrites exhibit a very regular rectangular shape perpendicular to the *c*-axis. As already reported for crystals grown by the Czochralski technique [7], the faceting occurs along {1 1 0} planes. The almost macroscopic arrangement of dendrites in domain-like regions seems to follow the growth rules set by its constituents. Neighboring domains of dendritic fresnoite were frequently observed to deviate only a few degrees in their respective orientation perpendicular to the growth direction. Particularly at lower growth rates, the implementation of large-angle grain boundaries seems to be energetically unfavorable.

The microstructure of the fresnoite glass-ceramics is the result of three subsequent crystallization steps. First, after nucleation in the vicinity of the cathode, due to the supercooling of the melt and the resulting negative temperature gradient in front of the growth plane, primary fresnoite crystals are formed by dendritic growth. During this dendritic crystallization, a considerable amount of solidification enthalpy is released, which in turn increases the temperature until the equilibrium liquidus temperature is reached. Dendrites do not form widely branching networks because some planes including (0 0 1) and {1 1 0} grow preferentially.

During the formation of primary (dendritic) fresnoite, the remaining melt is gradually enriched in SiO_2 until a eutectic concentration in the pseudo-binary system fresnoite-SiO_2 is adjusted. In the second step, the pseudo-binary eutectic fresnoite-silica solidifies lamellarly. The growth direction is opposite to the direction of heat removal. Therefore, the lamellae are always perpendicular to the surface of the primary fresnoite crystals.

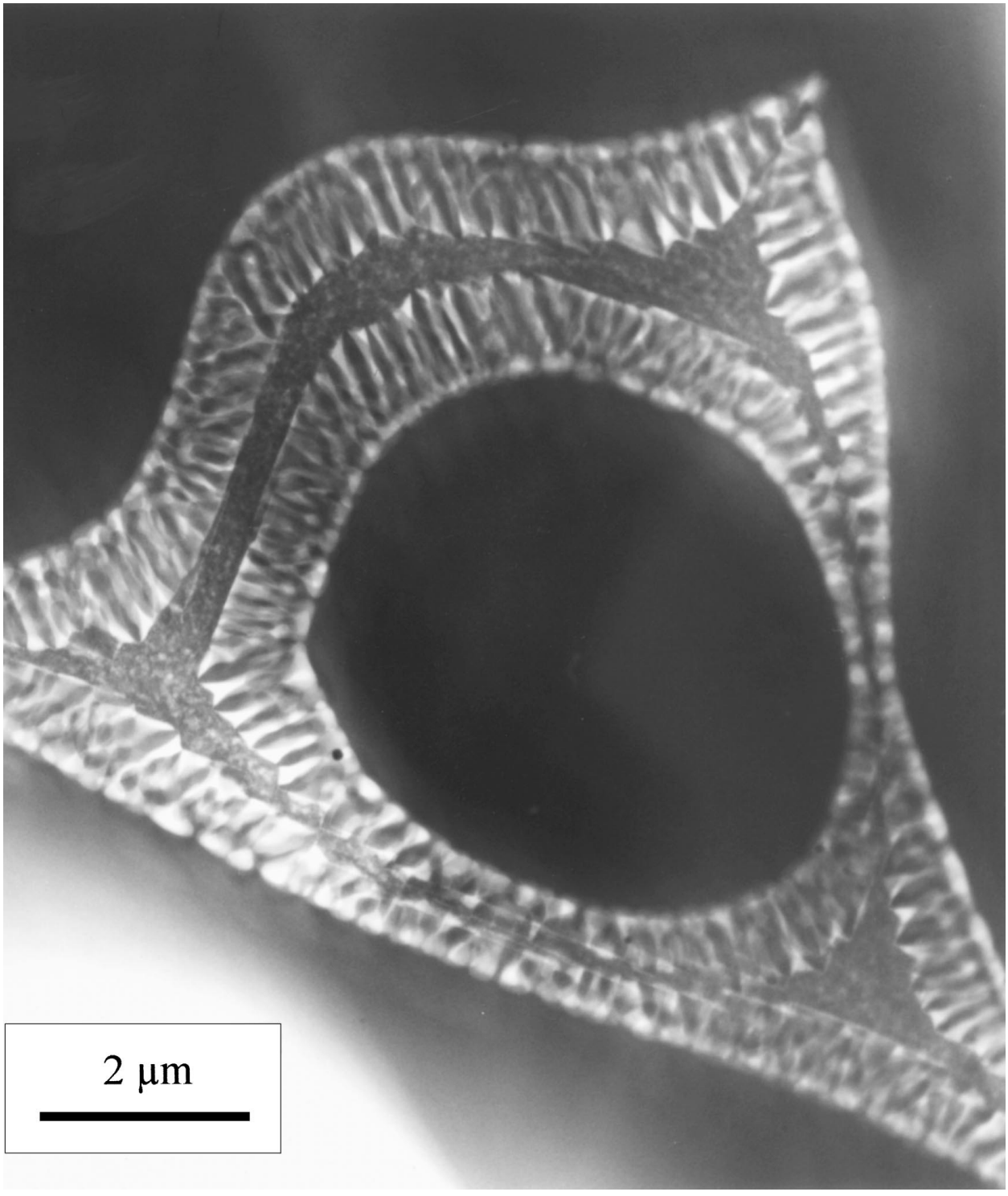

Figure 10 TEM micrograph recorded from the sample solidified at 1350 °C. Although the circular shape of the fresnoite dendrite in the middle is less typical, the lamellae (0.20 to 0.25 μm spaced) together with their backbone show what is generally observed in this sample.

The third step of the solidification process is dependent on the temperature and the possibilities of local heat removal, respectively. At temperatures of 1200 °C and 1350 °C, in the middle of the eutectic lamellae filling the interspaces of the dendritic branches, a lack of titanium builds up and therefore crystalline barium silicate, $Ba_5Si_8O_{21}$, and glassy silica are formed. An estimation of the volume fraction of the barium silicate phase showed that it is very unlikely that the absence of titanium in this remainder phase is a consequence of adding incorrect amounts of titania. In fact, the depletion of titanium along with the enrichment of silicon in these pockets might indicate the presence of Ti-enriched fresnoite as reported by Coats *et al*. [21].

In conjunction with this, the question arises as to where the Ti^{3+} formed at the cathode is to be found in the microstructure. Some features in the EELS data (particularly a pre-peak of the O K edge) acquired near the cathode indicate the presence of unoccupied hole states, which in turn are closely connected to oxygen stoichiometry. This is at least consistent with the assumption of Ti^{3+} incorporation in fresnoite (possibly preferred incorporation at Si positions?).

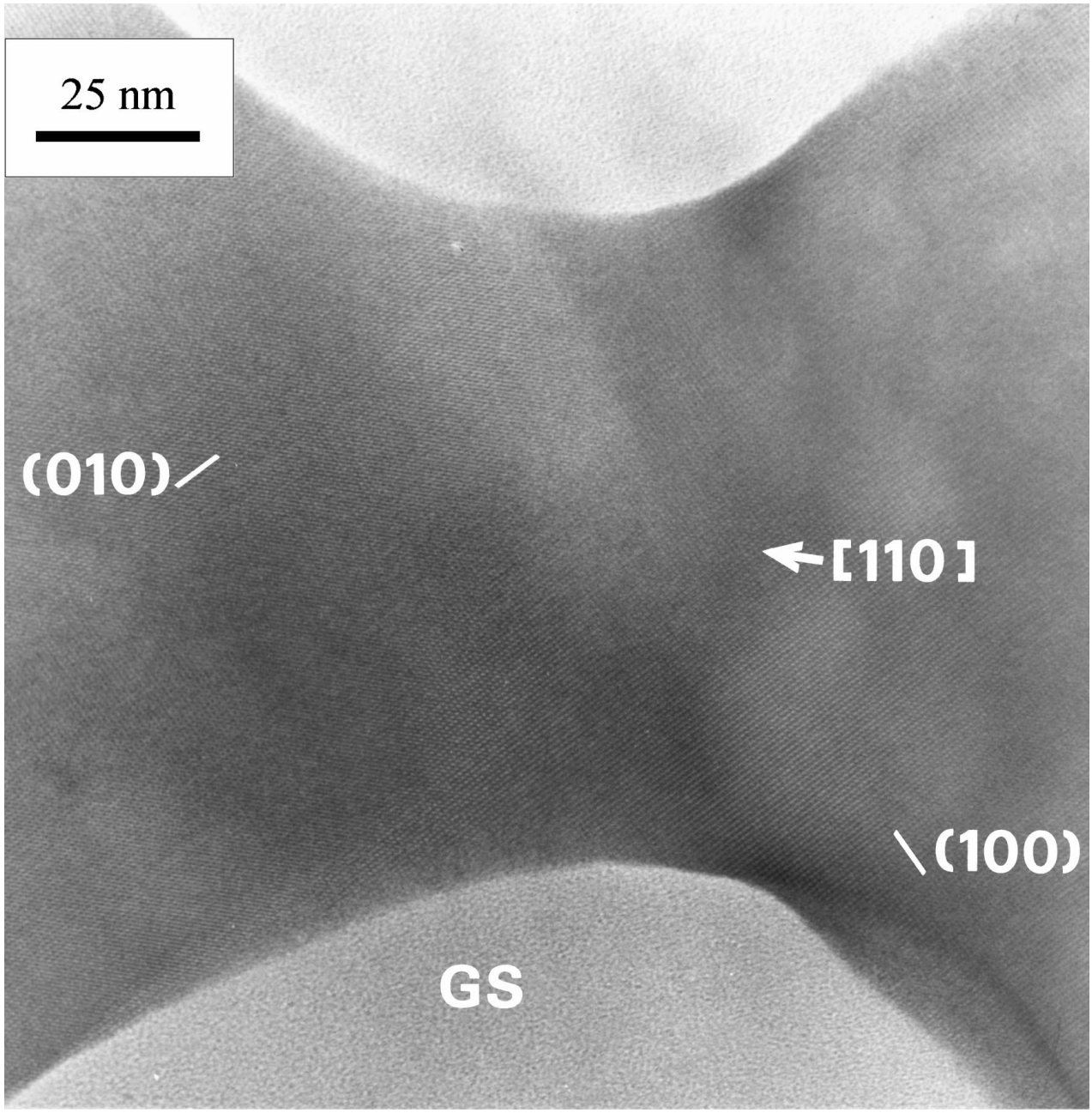

Figure 11 High resolution TEM (HRTEM) micrograph of the boundary between dendritic fresnoite (extending to the right) and one of the fresnoite lamellae (running to the left) in [0 0 1] projection. The continuation of lattice planes indicates that upon reaching the eutectic composition small protuberances in the fresnoite growth front initiate the growth of lamellar fresnoite. In the top and the bottom glassy silica (GS) is visible. As indicated by the lattice plane indices, also here the direction of lamellar growth follows {1 1 0}.

In the sample crystallized at 1150 °C, the lamellae structure of the eutectic is not as well-developed as in the other samples and frequently in the middle of the interspaces, a glassy phase occurs containing all elements necessary to form fresnoite. Due to the lower temperature, and hence decreasing diffusion coefficients, the formation of a crystalline phase is hampered since atoms are no longer able to reach their respective lattice sites.

The temperature of maximum crystal growth is much closer to the melting temperature than the temperature of maximum nucleation rate. This can be concluded from the shapes of the crystallized samples. On crystallizing at 1350 °C, seed formation predominantly takes place in the vicinity of the cathode near the surface (the temperature of which is slightly less than the temperature of the melt in the inner part of the sample). The somewhat decreased temperature in superficial regions of the melt results in smaller critical nuclei. Once nuclei of supercritical radii are formed, crystals grow rapidly into the melt resulting in a microstructure with almost all crystals originating from nucleation sites near the surface (the growth velocity at 1350 °C is almost at its optimum). Therefore, dendritic domains are much larger than in samples crystallized at lower temperatures. Halliyal *et al*. [8] took advantage of this effect by applying a steep temperature gradient to surface nucleated samples resulting in a closely neighboring region of seed formation and crystal growth, respectively.

In the other extreme, the sample solidified at 1150 °C, the temperature promotes the formation of seeds rather than being favorable for crystal growth. Therefore, the

microstructure consists of many small dendritic domains. Each domain originates from one of many nuclei formed along the cathode wire. Due to the decreased velocity of crystal growth, seeds also formed in the lower part of the sample can grow because growth fronts from the upper part (also here the temperature gradient will promote seed formation and subsequent growth in superficial regions) advance much more slowly than at 1350 °C. This effect was utilized by Ding *et al.* [16] who generated (by ultrasonic treatment with an aqueous solution of about 3.5 μm sized fresnoite particles) many seeds on the surface of the quenched glasses and subsequently heated the samples at temperatures between 760 and 900 °C.

In samples crystallized at different temperatures, the growth rate of the eutectic lamellae is different. This effect manifests itself in the lamellae spacing Λ of alternating layers of fresnoite and silica. At 1150 °C, a lamellae spacing of approximately 1 μm is observed, whereas already at 1200 °C Λ has about one third of this value. Since Λ is inversely proportional to the root of the growth rate, the temperature difference of 50 K already results in a growth rate which is ten times higher. The growth rate at 1350 °C is—due to a Λ of about 0.2 to 0.25 μm—about 25 times higher than at 1150 °C.

Summarizing the above-mentioned influence of the solidification temperature on the microstructure, it appears that the most effective orientation in radial direction can be achieved at 1150 °C due to the high nucleation rate and the rather low crystal growth rate. The microstructure at this temperature consists of relatively small dendritic domains, the lamellar solidification of the quasi-binary eutectic fresnoite-silica is only indicated and there is no formation of a second crystalline phase in the middle of dendritic fresnoite branches.

Glass-ceramics showing a high degree of grain orientation in the radial direction are of little practical use. The fabrication of parallel-aligned grains would be much more relevant. Knowing the influence of the solidification temperature on the microstructure will also allow us to prepare fresnoite glass-ceramics with parallel grain orientation. In this case, a cathode plate or even a suitably constructed hole mask, rather than a wire, have to be used for electrochemically induced crystallization at 1150 °C. Work on this geometry as well as application of the technique to other system, including $Sr_2TiSi_2O_8$, $Ba_2TiGe_2O_8$ and $LiNbO_3$, are in progress. Investigation of the resulting microstructures will lead to a deeper understanding of the mechanism of electrochemically induced nucleation.

5. Conclusions

A novel technique of electrochemically induced nucleation allows us to fabricate glass-ceramics with outstanding grain orientation. An electric current is flowed through a supercooled fresnoite-silica melt. Electrons emitted from the cathode cause nucleation at the cathode. The high degree of orientation is subsequently attained by growth selection among crystals growing from these seeds into the melt.

In this study, the dependence of the microstructure on the temperature of solidification was investigated. Samples were prepared at 1150 °C, 1200 °C as well as 1350 °C.

The solidification is a three-stage process. First, dendritic fresnoite—being arranged in domain-like structures—is formed leaving a quasi-binary eutectic fresnoite-silica. The diameter of the dendritic branches is almost independent of the temperature of crystallization. Fresnoite-silica eutectic in the interspaces solidifies lamellarly with alternating crystalline fresnoite and glassy silica. Depending on the temperature of solidification (and hence the growth rates), the lamellae are well developed (1350 °C and 1200 °C) or only indicated (1150 °C). Surrounded by lamellar eutectic, in the interspace between fresnoite dendrites a third phase is formed. At 1150 °C, this phase is glassy and possesses the composition of the initial melt. By contrast, in the samples solidified at 1200 °C and 1350 °C, this phase consists of glassy silica and crystalline $Ba_5Si_8O_{21}$.

Specimens prepared at 1350 °C, due to the dependence of nucleation and growth rate on the temperature of solidification exhibit a microstructure consisting of coarse dendritic domains and consequently a lower degree of radial texturing whereas samples crystallized at 1150 °C distinguish themselves by a high number of radially well oriented dendritic domains.

Acknowledgements

The authors would like to thank Dr G. Völksch for his kind assistance in scanning electron microscopy and Dr H.-J. Kleebe, University of Bayreuth, who performed the PEELS measurements. This work was supported by Deutsche Forschungsgemeinschaft (DFG), Bonn Bad Godesberg (Germany).

References

1. J. T. ALFORS, M. C. STINTON, R. A. MATTHEWS and A. PABST, *Am. Mineral.* **50** (1965) 314.
2. R. MASSE, J.-C. GRENIER and A. DURIF, *Bull. Soc. Fr. Mineral. Cristallogr.* **90** (1967) 20.
3. P. B. MOORE and J. LOUISNATHAN, *Z. Kristallog.* **130** (1969) 438.
4. "Numerical Data and Functional Relationships in Science and Technology," Vol. III 7d 1α (Landolt-Börnstein, Springer, Berlin) p. 306.
5. S. A. MARKGRAF, A. HALLIYAL, A. S. BHALLA, R. E. NEWNHAM and C. T. PREWITT, *Ferroelectrics* **62** (1985) 17.
6. A. HALLIYAL, A. S. BHALLA, S. A. MARKGRAF, L. E. CROSS and R. E. NEWNHAM, *ibid.* **62** (1985) 27.
7. H. SCHMID, P. GENEQUAND, H. TIPPMANN, G. POUILLY and H. GUEDU, *J. Mater. Sci.* **13** (1978) 2257.
8. A. HALLIYAL, A. S. BHALLA, R. E. NEWNHAM and L. E. CROSS, *ibid.* **16** (1981) 1023.
9. P. S BECHTHOLD, S. HAUSSÜHL, E. MICHAEL, J. ECKSTEIN, K. RECKER and F. WALLRAFEN, *Phys. Lett. A* **65** (1978) 453.
10. M. KIMURA, *J. Appl. Phys.* **48** (1977) 2850.
11. S. HAUSSÜHL, J. ECKSTEIN, K. RECKER and F. WALLRAFEN, *J. Cryst. Growth* **40** (1977) 200.
12. R. Y. TING, A. HALLIYAL and A. S. BHALLA, *Appl. Phys. Lett.* **44** (1984) 852.
13. A. HALLIYAL, A. SAFARI, A. S. BHALLA, R. E. NEWNHAM and L. E. CROSS, *J. Am. Ceram. Soc.* **67** (1984) 331.

14. A. HALLIYAL, A. SAFARI, A. S. BHALLA and R. E. NEWNHAM, *Ferroelectrics* **50** (1983) 45.
15. A. HALLIYAL, A. S. BHALLA, R. E. NEWNHAM and L. E. CROSS, *J. Mater. Sci.* **16** (1981) 1023.
16. Y. DING, Y. MIURA and A. OSAKA, *J. Am. Ceram. Soc.* **77** (1994) 2905.
17. Y. LI, B. S. CHAO and H. YAMAUCHI, *J. Appl. Phys.* **71** (1992) 4903.
18. R. KEDING and C. RÜSSEL, *Ber. Bunsenges. Phys. Chem.* **100** (1996) 1515.
19. C. RÜSSEL and R. KEDING, *J. Non-Cryst. Solids* **219** (1997) 136.
20. T. HÖCHE, H.-J. KLEEBE, R. KEDING and R. BRYDSON, in preparation.
21. A. M COATS, N. HIROSE, J. MARR and A. R. WEST, *J. Solid State Chem.* **126** (1996) 105.

Received 17 August
and accepted 18 August 1998